remote sensing

MDPI

Article

A Universal Method for Quantitatively Measuring Land Surface Anomaly Intensity Using Multiscale Remote Sensing Features

Shiying Gao [1,2], Jinshui Zhang [1,2,*], Yaming Duan [1,2] and Qiao Wang [2]

[1] State Key Laboratory of Remote Sensing Science, Beijing Normal University, Beijing 100875, China; 202321051188@mail.bnu.edu.cn (S.G.)
[2] Institute of Remote Sensing Science and Engineering, Faculty of Geographical Science, Beijing Normal University, Beijing 100875, China
* Correspondence: zhangjs@bnu.edu.cn

Abstract: Land surface anomalies refer to various activities on the Earth's surface that consist of short-term and sudden changes due to external disturbances. These anomalies are closely related to the safety of human life and property. Remote sensing offers irreplaceable advantages such as broad coverage, high temporal dynamics, and comprehensive observations, so it is the most effective tool for monitoring land surface anomalies and measuring their intensities. However, existing studies have limitations such as unclear sensitivity features, uncertain applicability, and a lack of quantitative expression at different scales. Therefore, this study develops a quantitative assessment framework for land surface anomaly intensity across four scales: the pixel scale, structure scale, object scale, and scene scale. This framework enables an adaptive and flexible weight determination of the intensity of land surface anomalies from a satellite perspective. Using the Chongqing fire as an example of a land surface anomaly, this study evaluates its land surface anomaly intensity. Moreover, we demonstrate the method's applicability to other land surface anomaly events, such as floods and earthquakes. The experiments reveal that the land surface anomaly intensity evaluation framework, which is constructed based on pixel-scale, structure-scale, object-scale, and scene-scale features, can quantitatively express the land surface anomaly intensity with an accuracy of 75.25% and more effectively represent severely affected areas. The weights of the features at the four scales sequentially decrease: structure scale (0.2974), pixel scale (0.3225), object scale (0.1867), and scene scale (0.1932). The extensive application of this method to other land surface anomaly events provides accurate quantitative expressions of the land surface anomaly intensity. This remote sensing-based multiscale feature assessment method is adaptable and applicable to various land surface anomalies and offers critical decision support for land surface anomaly intensity warning systems.

Keywords: land surface anomaly intensity; remote sensing; multiscale features; entropy weight method

check for updates

Citation: Gao, S.; Zhang, J.; Duan, Y.; Wang, Q. A Universal Method for Quantitatively Measuring Land Surface Anomaly Intensity Using Multiscale Remote Sensing Features. *Remote Sens.* **2024**, *16*, 4397. https://doi.org/10.3390/rs16234397

Academic Editor: Melanie Vanderhoof

Received: 2 October 2024
Revised: 20 November 2024
Accepted: 22 November 2024
Published: 24 November 2024

Copyright: © 2024 by the authors. Licensee MDPI, Basel, Switzerland. This article is an open access article distributed under the terms and conditions of the Creative Commons Attribution (CC BY) license (https://creativecommons.org/licenses/by/4.0/).

1. Introduction

Land surface anomalies refer to "the sudden phenomenon threatening the natural or social environment, which destroys the stable balanced state of the Earth's surface conforming to the historical evolutionary law caused by the single or double influence of natural and human factors" [1]. Land surface anomalies are characterized by suddenness, diversity, randomness, and complexity. In recent years, the Earth has experienced a surge in sudden land surface anomalies caused by both natural factors and human activities. These events, including earthquakes, floods, landslides, other natural disasters, environmental pollution, ecological degradation, safety incidents, and unauthorized development, have become increasingly frequent. They are characterized by widespread distribution, high occurrence rates, rapid evolution, extensive impact, and significant economic losses [2]. The demands for disaster relief, environmental emergency response, and environmental regulatory oversight in recent years have created a substantial need for early warning

systems for land surface anomalies. This demand has driven the development of methods for generating land surface anomaly intensities [3–5]. A timely assessment of land surface anomaly intensities is crucial for decision-makers to effectively implement macroscale control; strategically allocate human, material, and financial resources; and minimize damage to the natural environment, life, and property caused by these anomalies. Thus, timely assessment supports prompt and effective disaster relief efforts.

Land surface anomaly intensity can be defined as the extent of damage to the land surface caused by anomalies. The intensity of a disaster is determined by two fundamental factors: the intensity of the disaster-causing factors and the density of the population and economy in the affected areas. The latter represents the capacity of an area to defend against and withstand a disaster [6]. Traditional methods for assessing land surface anomaly intensity often rely on postevent ground surveys. While highly accurate, this method is heavily influenced by subjective human judgement. Moreover, this method requires significant time and labour and suffers from time delays, so it is less effective for real-time decision-making [7,8]. Remote sensing-based land surface anomaly intensity detection is assessed by analysing the spectral, radiative, and textural features of satellite images, which can quantitatively reflect land surface anomalies. This approach involves extracting comprehensive features and determining thresholds or simply extracting the attributes of land surface anomalies to translate satellite remote sensing features into actionable knowledge about land surface anomaly intensity.

Remote sensing enables the large-scale monitoring of land surface anomalies and provides abundant, reliable data for detecting land surface anomaly intensities [9–12]. The common methods used in recent years include manual interpretation [13,14], geographic object-based image analysis (GEOBIA) [15–17], remote sensing indicator-based methods, and machine learning methods [18,19]. Among these methods, remote sensing indicator-based methods are the most commonly used; they do not require ground truth data, are fast, and offer high accuracy. Remote sensing indexes are significant indicators. Commonly used indexes are the Forel–Ule Index (FUI) [20], normalized difference vegetation index (NDVI) [21], Modified Normalized Difference Water Index (MNDWI) [22], and Leaf Area Index (LAI) [23]. Land surface anomaly intensity can be assessed by analysing the index itself or calculating the index difference before and after the anomaly. In addition, the intensities of land surface anomalies can also be assessed via several indicators that are directly detected via remote sensing, such as surface deformation [24], total suspended solids (TSSs) [25], and the water level [26]. All of these existing methods have limitations, such as unclear sensitivity features, uncertain applicability, and a lack of quantitative expression at different scales. These shortcomings hinder their ability to support decision-making for land surface anomaly warning systems. Therefore, it is imperative to develop a comprehensive remote sensing feature system to measure land surface anomaly intensity quantitatively and refine the theoretical framework.

Given the aforementioned challenges, this paper first proposes a universal land surface anomaly intensity assessment method using multiscale remote sensing features. We develop an evaluation framework to measure the land surface anomaly intensity, where we select the Chongqing fire as a typical case to analyse the relationship between land surface changes and remote sensing feature changes. We establish an index system to quantitatively assess the land surface anomaly intensity across multiple scales, including the pixel scale, structure scale, object scale, and scene scale, which are defined from the viewpoint of satellites. Instead of using only the pixel or structure scale, we consider four scales to fully use the remote sensing image information. Furthermore, we explore the weight distributions of multiscale features to evaluate the land surface anomaly intensity via the entropy weight method. The feature weights are only determined based on remote sensing data without the need for additional expert knowledge or manual intervention. Therefore, we can automatically obtain the land surface anomaly intensity. This paper aims to construct a quantitative evaluation model, analyse the sensitive remote sensing features of land surface anomaly intensity, elucidate the intrinsic relationship between

land surface anomaly intensity and remote sensing features, and validate the applicability of the proposed remote sensing measurement framework across various types of land surface anomalies.

2. Remote Sensing Framework for Measuring Land Surface Anomaly Intensity

2.1. Definition of Land Surface Anomaly Intensity

Land surface anomaly intensity is defined as the degree of deviation from the normal state of the Earth's surface, where "normal" refers to the stable and persistent status and properties of land surface features over an extended period. The remote sensing warning of land surface anomaly intensity involves the detection of land surface anomalies and the analysis of spectral, radiative, scattering, geometric, and textural features. These features are used to identify diagnostic feature thresholds and composite indexes for anomalies and translate satellite imagery data into actionable knowledge of the land surface anomaly intensity [1]. Based on this definition, pre-anomaly remote sensing characteristics can be considered normal values, and post-anomaly characteristics can be considered anomalous values. The change between these values is used as an input to evaluate the land surface anomaly intensity.

The remote sensing-based land surface anomaly intensity detection framework is in Figure 1. The pixel is the basic unit of remote sensing imagery. At the pixel scale, the degree of change in physical characteristics, such as the tone of the land surface features, can reflect individual differences. Land surface anomaly intensity is generated from the degree of radiative brightness changes. The structure scale captures the greyscale changes between pixels and their surroundings. Changes in physical characteristics such as land surface roughness and smoothness are measurements of land surface anomaly intensity. At the object scale, the information of relatively independent pixel sets is conveyed into features such as the state, fragmentation, shape, and size of anomalous pixel patches in a four or eight neighbourhood, which are indicators of the land surface anomaly intensity. The scene scale captures the magnitude of the anomaly over a defined spatial area, which expresses the spatial positions and relationships of objects. It can reflect geometric characteristics such as the size of the anomaly areas, which can be quantified as the land surface anomaly intensity at the scene scale.

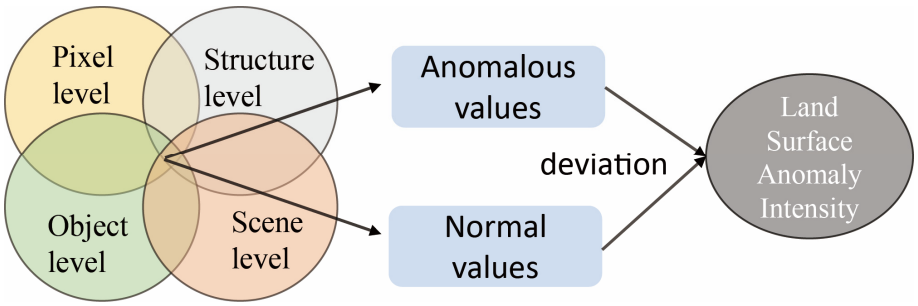


Figure 1. Diagram of remote sensing-based land surface anomaly intensity detection.

2.2. Mathematical Model for Measuring Land Surface Anomaly Intensity

The formula for calculating the land surface anomaly intensity is defined as follows:

$$LSAI = PI \otimes SI \otimes OI \otimes LI \quad (1)$$

where *LSAI* is the land surface anomaly intensity, *PI* is the pixel intensity, *SI* is the structure intensity, *OI* is the object intensity, and *LI* is the landscape intensity. (To differentiate from structure intensity (*SI*), "Landscape" is used here instead of "Scene." However, the "scene scale" will continue to be used in subsequent sections).

(1) Pixel-Scale Land Surface Anomaly Intensity

The features used to assess the intensity at the pixel scale include spectral and scattering features. Spectral features, which are crucial in remote sensing imagery, describe the statistical characteristics of pixels across various bands. Common spectral features include brightness values, standard deviations, and others. Differences in spectral features can reflect changes in the physical properties of land cover caused by land surface anomalies, such as colour. Greater differences correspond to greater land surface anomaly intensities. Common scattering characteristics include radar backscatter coefficients, which can effectively capture changes in physical properties such as surface roughness. The magnitude of change in these features is directly proportional to the land surface anomaly intensity. The calculation formula for the *PI* (pixel intensity) is defined as follows:

$$PI = L \otimes S \tag{2}$$

where L denotes spectral features, and S denotes scattering features.

(2) Structure-Scale Land Surface Anomaly Intensity

The features used to assess the intensity at the structural scale are texture and variance. Texture refers to the frequency of tonal variations in land cover and is an essential feature that reflects structural information on the land surface. The variance, which is the sum of the squared differences between the pixel values and the mean, indicates the degree of dispersion of the pixel values. Differences in texture and variance can effectively capture changes in physical properties caused by surface anomaly events, such as the roughness and smoothness of the land surface. The magnitude of these feature changes can further reflect the land surface anomaly intensity. The calculation formula for the *SI* (structure intensity) is defined as follows:

$$SI = T \otimes V \tag{3}$$

where T is texture, and V is variance.

(3) Object-Scale Land Surface Anomaly Intensity

Object-scale features consider the differences between land surface anomaly patches and are a synthesis of information about the land surface anomaly intensity. The assessment of intensity at the object scale relies on the geometric characteristics of the anomaly area. Among these, the fragmentation feature is a key geometric characteristic that effectively contributes to the evaluation of the land surface anomaly intensity. The boundary fragmentation of the anomaly area can be expressed using the edge ratio, which is calculated as the ratio of the object perimeter to the object area. A greater edge ratio corresponds to a more fragmented anomaly area, which results in a lower land surface anomaly intensity. Additionally, the object area can represent the land surface anomaly intensity at the object scale: a larger object area corresponds to a more continuous impact of the anomaly event and a greater land surface anomaly intensity. The calculation formula for the Object Intensity (*OI*) is defined as follows:

$$OI = E \otimes A \tag{4}$$

where E is the edge ratio, and A is the area.

(4) Scene-Scale Land Surface Anomaly Intensity

The scene scale is the most macroscopic scale of the land surface anomaly intensity. At the scene scale, the intensity is relative to a variable range. The scene-scale features used to evaluate the scene-scale land surface anomaly intensity are the area ratio and count, which are defined on a predesigned grid. The area ratio is the proportion of the anomalous area in a unit grid. A larger area ratio generally indicates a longer duration and a broader impact of the land surface anomaly event, which correlates with a higher land surface anomaly intensity. The count is the number of surface anomaly locations; a

greater number of locations corresponds to a greater land surface anomaly intensity. The calculation formula for the landscape intensity (*LI*) is as follows:

$$LI = P \otimes N \tag{5}$$

where P is the proportion of the anomaly area in a unit grid (area ratio), and N is the number of surface anomaly locations (count).

The land surface anomaly intensity evaluation model is in Figure 2. With this model, it is possible to achieve multiscale quantitative assessments of land surface anomaly intensity.

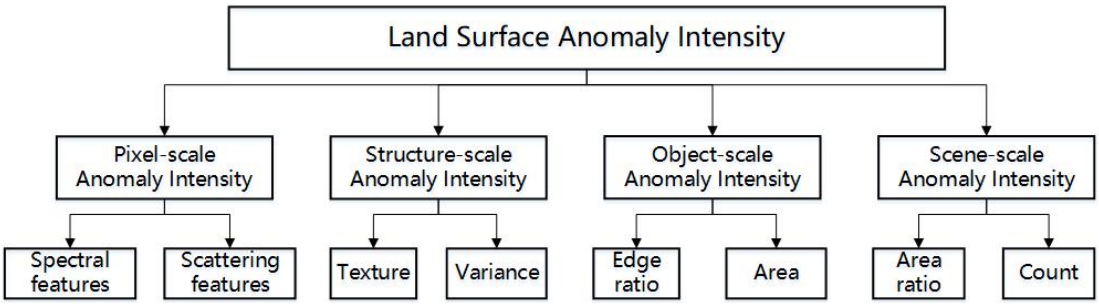


Figure 2. Land surface anomaly intensity evaluation model.

3. Experimental Design

- Study Area

The study area is located in the Jinyun Mountain region in Chongqing, China, within the geographical coordinates of 29°45′–29°48′N and 106°18′–106°22′E. A fire event occurred in this area from 21 to 26 August 2022, affecting a total area of 13.98 km^2. Owing to the dense vegetation in the mountainous region, the fire rapidly spread, persisted for an extended period, and caused severe damage to forest resources in the Jinyun Mountain region. The safety, property, and livelihoods of surrounding village residents were also severely impacted. The Chongqing fire fits the definition of a land surface anomaly, which makes it a typical example of a land surface anomaly event. The conclusions obtained from the Chongqing fire data are universal for various land surface anomalies. The study area is illustrated in Figure 3, where the remote sensing image is a true-colour image captured by Sentinel-2 on 24 August 2022. The method of integrating remote sensing and spatial features was used to extract the burned area [27]. Additionally, ground truth labels for the land surface anomaly intensity are depicted in Figure 3.

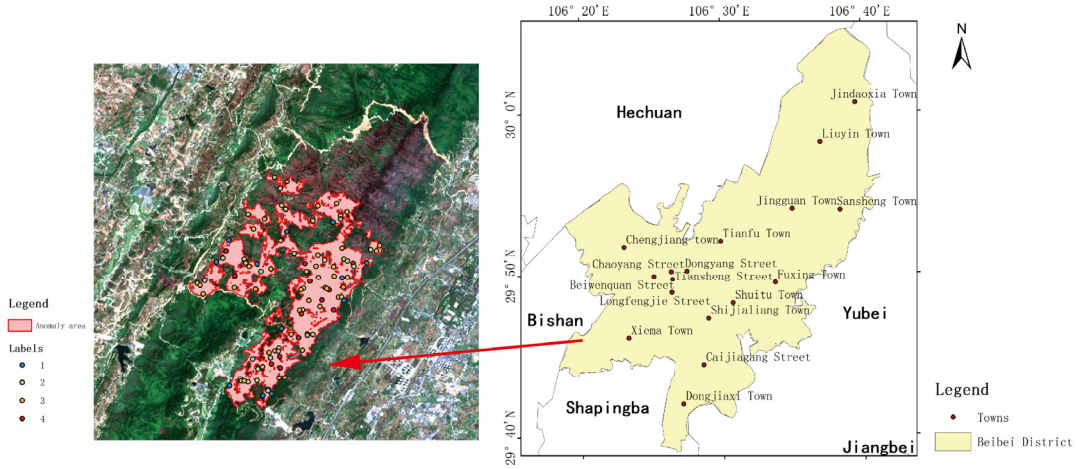


Figure 3. Study area. The **left** image shows the geographical location of the study area. The **right** image shows the Sentinel-2 image of the study area. The red polygon is the anomaly area, and the points are labelled with the true land surface anomaly intensity class determined by humans.

- Research Data and Standardization Processing

The data in this study include Sentinel-2 and Sentinel-1 remote sensing data. Sentinel-1 and Sentinel-2 are Earth observation satellites that are part of the global monitoring initiative "Copernicus Programme", which provides high-resolution multispectral and radar imaging of the Earth's surface. To fully reflect the land surface changes, two Sentinel-2 multispectral images and two Sentinel-1 SAR images covering the study area were selected for this study. These images were captured at two time points: before and during the land surface anomaly event. Detailed information on these images is provided in Table 1. The Sentinel-2 multispectral image captured on 24 August 2022 was used to determine the anomaly area [27]. Based on the anomaly area, the object-scale features and the scene-scale features can be further analysed. The two Sentinel-1 SAR images were used to extract scattering features, and the two Sentinel-2 multispectral images were used to extract spectral and structural features.

Table 1. List of image data for study area.

ID Number	Satellite	Remote Sensing Image Acquisition Dates
1	Sentinel-2	11 August 2022
2	Sentinel-2	24 August 2022
3	Sentinel-1	11 August 2022
4	Sentinel-1	28 August 2022

- Remote Sensing Feature System for Fire Intensity Assessment

Taking the Chongqing fire as a representative example of a land surface anomaly, we developed a remote sensing feature system to assess fire intensity. Existing online fire detection services such as FIRMS and SaaS can provide real-time active fire locations but do not provide their intensities, whereas the system we developed can provide intensities. This system is based on the model of the land surface anomaly intensity and incorporates features across four scales: pixel, structure, object, and scene.

- Pixel Scale

Fires cause significant damage to healthy vegetation and cause buildings to collapse, which substantially changes the physical properties of the land surface. A greater fire intensity causes more pronounced physical changes, which are reflected in the observed differences in remote sensing features. Therefore, fire intensity can be defined as the extent to which features in the affected area deviate from their normal state. Based on this concept, the absolute differences in feature values before and after the fire in the fire-affected area can be used as input features to reflect the fire intensity. In this study, we selected spectral and scattering features to assess the fire intensity. The absolute differences in these features were calculated using imagery from before and during the fire.

(1) Spectral features

Spectral features include the absolute differences in the red band (dRED), green band (dGREEN), blue band (dBLUE), near-infrared band (dNIR), and two shortwave infrared bands (dSWIR1, dSWIR2). Three remote sensing indexes were considered: the difference in normalized vegetation index (dNDVI), difference in burned area index (dBAR), and difference in normalized burn ratio (dNBR). dRED, dGREEN, and dBLUE can effectively reflect changes in the physical properties of the land surface, such as colour, whereas dNIR is susceptible to differences between burned areas and healthy vegetation, so it is an effective indicator of the extent of fire damage. dSWIR1 and dSWIR2 have a certain penetration ability through smoke, which is useful in mitigating the impact of smoke on fire assessments. In addition, flames have significantly higher pixel values in the shortwave infrared bands than other land surface features do; thus, the absolute differences in the shortwave infrared bands before and after a fire can be used to assess the fire intensity

better. The destruction of vegetation after a fire results in a noticeable decrease in the NDVI, so the dNDVI is a useful indicator of fire intensity [23]. The BAR index, which enhances post-fire surface information using the red and near-infrared bands, significantly increases in burned areas and clearly deviates from the "normal" state of the surface. Similarly, the NBR value significantly decreases after a fire, and this deviation is useful in fire intensity assessments. Additionally, the normalized burn ratio (NBR) can help reduce the impact of smoke, which may obscure observations in the early stages of a fire [28].

(2) Scattering features

Scattering features include the VV- and VH-polarized radar backscatter coefficients [29]. After a fire, vegetation is destroyed, which significantly changes the image texture. The VV- and VH-polarized radar backscatter coefficients can effectively reflect changes in the roughness and smoothness of the land surface and provide further insights into the land surface anomaly intensity.

- Structure Scale

At the structure scale, similar to the pixel scale, changes in the physical properties of the land surface alter texture features. A greater fire intensity corresponds to more pronounced texture differences. Therefore, the absolute differences in texture features before and after a fire can be used as input structural features to assess the structural fire intensity. These differences are calculated via imagery from before and during the fire.

The greyscale co-occurrence matrix (GLCM) is widely used in disaster intensity assessments because it effectively reflects the texture characteristics of an image [30,31]. In this study, we selected the absolute differences of four GLCM characteristics to describe the texture differences between pre-fire and post-fire images: the absolute difference in entropy (dEntropy), the absolute difference in energy (dEnergy), the absolute difference in contrast (dContrast), and the absolute difference in correlation (dCorrelation). We used the near-infrared bands of pre- and post-fire images to calculate entropy, energy, contrast, and correlation before and after the fire and calculated the absolute value of the difference to obtain dEntropy, dEnergy, dContrast, and dCorrelation. Entropy reflects the complexity of the greyscale distribution in an image, energy indicates the coarseness of the texture, contrast represents the depth of texture grooves, and correlation measures the similarity of greyscales in the row or column directions.

In addition to the GLCM, variance can reflect surface roughness and smoothness. The absolute difference in variance (dVariance) can similarly be used to assess fire intensity. By integrating these five features, a comprehensive representation of the changes in image texture characteristics can be obtained.

- Object Scale

Fragmentation features are key characteristics of burned areas and can reflect the development of fires. A greater fragmentation of burned areas indicates a greater discontinuity of fire development and corresponds to a lower fire intensity. In this study, the fire intensity at the object scale was assessed using two fragmentation features, the edge ratio and the area, which can be calculated through the anomaly area.

The edge ratio is defined as the ratio of the perimeter to the area of a burned area. A higher edge ratio suggests a greater fragmentation of the burned area and implies a lower fire intensity. The area refers to the size of the burned area. A larger area indicates a larger affected area, which corresponds to a higher fire intensity.

- Scene Scale

Since this study only focuses on a single land surface anomaly event, specifically a fire, at a single location, the count within the scene-scale features remains consistent across the entire affected area. Therefore, only the area ratio is selected as a scene-scale feature for the fire intensity assessment. This feature is defined by constructing a grid with a resolution of 0.5 km $\times$ 0.5 km in the study area and calculating the ratio of the burned area in a grid to

the grid area. A higher area ratio indicates a larger and continuous area affected by the fire and a higher fire intensity.

Based on the selected features across the four scales, a remote sensing feature system for fire intensity assessment was constructed, as shown in Figure 4.

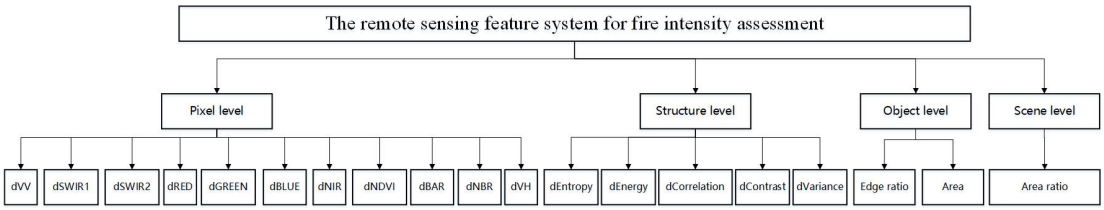


Figure 4. Remote sensing feature system for fire intensity assessment.

- Measurement of Fire Intensity

Based on the remote sensing feature system for fire intensity assessment, the entropy weight method was used to calculate the weights of each feature at different scales and the weights of the anomaly intensity for each scale. A higher feature variance corresponds to a larger feature weight. The basic steps are as follows:

(1) Feature Normalization

The features are first normalized. Here, x_{ij} is the value of the jth feature in the ith sample, y_{ij} is the normalized value of the jth feature in the ith sample, x_j is the jth feature, and *Max* and *Min* denote the maximum and minimum values, respectively. For positive features, normalization is performed via Formula (6); for negative features, Formula (7) is applied.

$$y_{ij} = \frac{x_{ij} - Min(x_j)}{Max(x_j) - Min(x_j)} \tag{6}$$

$$y_{ij} = \frac{Max(x_j) - x_{ij}}{Max(x_j) - Min(x_j)} \tag{7}$$

(2) Feature Weight Calculation

The feature proportion is calculated, where p_{ij} is the feature proportion, and n is the sample size, which is equal to the number of pixels.

$$p_{ij} = \frac{y_{ij}}{\sum_{i=1}^{n} y_{ij}} \tag{8}$$

(3) Entropy Calculation

The entropy value is calculated, where E_j is the entropy value for the jth feature, p_{ij} is the feature proportion, and n is the sample size.

$$E_j = -k\sum_{i=1}^{n} p_{ij} \cdot lnp_{ij},\ k = \frac{1}{ln\ n} \tag{9}$$

(4) Feature weight calculation

Then, the weight w_j for the jth feature is determined, where m is the total number of features.

$$w_j = \frac{1 - E_j}{\sum_{j=1}^{m}(1 - E_j)} \tag{10}$$

Based on the calculated feature weights at each scale, a weighted composite score is obtained for each scale.

$$p = \sum_{j=1}^{m}(w_j \times y_{ij}) \tag{11}$$

where p is the intensity for a scale, y_{ij} is the normalized feature value, and w_j is the corresponding weight of the jth feature at that scale.

Finally, the weights for the pixel, structure, object, and scene scales are calculated via the entropy weight method, and these weights are integrated to generate the land surface anomaly intensity.

$$P = p_{\text{pixel}} \times w_{\text{pixel}} + p_{\text{structure}} \times w_{\text{structure}} + p_{\text{object}} \times w_{\text{object}} + p_{\text{scene}} \times w_{\text{scene}} \quad (12)$$

where p_{pixel} is the intensity of the pixel scale, $p_{structure}$ is the intensity of the structure scale, p_{object} is the intensity of the object scale, and p_{scene} is the intensity of the scene scale. Similarly, w_{pixel} is the weight of the pixel scale, $w_{structure}$ is the weight of the structure scale, w_{object} is the weight of the object scale, and w_{scene} is the weight of the scene scale.

- Accuracy Assessment

The accuracy of the fire intensity assessment is evaluated using a confusion matrix. Based on the pre-fire and post-fire Sentinel-2 images of the study area, 101 label points were randomly selected in the burned area, as shown in Figure 3. The land surface anomaly intensities of these label points were extracted and classified using an equal interval classification method. In this study, the intensity scales were categorized as follows: 0–0.25 as level 1, 0.25–0.5 as level 2, 0.5–0.75 as level 3, and 0.75–1 as level 4.

Since there is no truth value of the land surface anomaly intensity, we considered the intensities obtained by manual inspection as the truth values. We propose land surface characteristics and remote sensing characteristics for different fire intensity levels in Table 2. Despite the subjectivity of manual inspection methods, for land surface anomaly intensities that have no true value, these characteristics match our understanding, and we believe that they can reflect the relative severity of the land surface anomaly. According to Table 2, the true intensity levels of these label points were visually determined via manual inspection.

Table 2. Information on different fire intensity classes.

Class	Land Surface Characteristics	Remote Sensing Characteristics
1	There are no significant changes in land cover.	The areas appear grey–green and green, mostly located around the perimeter of the burned area.
2	A small portion of the surface features is partially unburned.	The areas appear grey–green with small patches of dark purple.
3	Most of the surface features have been completely burned.	The areas appear black with scattered patches of light grey and dark green.
4	The surface vegetation is completely destroyed.	The areas appear black and deep purple.

A confusion matrix was subsequently constructed to calculate the classification accuracy. The formula for accuracy calculation is as follows:

$$Accuracy = \frac{T}{N} \quad (13)$$

where $Accuracy$ is the classification accuracy, T is the number of correctly classified label points, and N is the total number of label points.

4. Results and Analysis

- Remote Sensing Evaluation Results and Analysis of Fire Intensity

The weights of the features across different scales, i.e., pixel-scale, structure-scale, object-scale, and scene-scale features, were determined using the entropy weight method, as shown in Table 3. Among the four scales, the weights decrease in the order of structure scale, pixel scale, scene scale, and object scale. This finding indicates that pixel-scale and

structure-scale features more significantly contribute to the assessment of fire intensity, whereas object-scale and scene-scale features contribute relatively less.

Table 3. Weights of fire intensity assessment feature system.

Pixel Scale		**Structure Scale**		**Object Scale**		**Scene Scale**	
Weight: 0.2974		**Weight: 0.3225**		**Weight: 0.1867**		**Weight: 0.1932**	
Features	**Weight**	**Features**	**Weight**	**Features**	**Weight**	**Features**	**Weight**
dRED	0.1848	dContrast	0.2832	Edge ratio	0.0004	Area ratio	1.0
dGREEN	0.0226	dEntropy	0.1731	Area	0.9996		
dBLUE	0.0469	dEnergy	0.1969				
dNIR	0.00002	dCorrelation	0.1752				
dSWIR1	0.0652	dVariance	0.1716				
dSWIR2	0.4707						
dNDVI	0.0243						
dBAR	0.0545						
dNBR	0.0287						
dVV	0.0536						
dVH	0.0486						

The larger weights of the pixel-scale and structure-scale features can be attributed to the following factors: For the pixel-scale features, the transition of surface colours from green to dark purple and black post-fire indicates significant changes in land cover, which can be effectively captured by spectral features. Additionally, the burning of vegetation causes noticeable changes in remote sensing indexes such as the normalized difference vegetation index (NDVI), and more intense fires lead to more pronounced changes. For the structure-scale features, the destruction of forests due to fire results in significant texture changes, which are also more evident in areas with higher fire intensities.

Moreover, the lower weights of the object-scale and scene-scale features may be due to the following reasons. These features aggregate information at a larger scale. The burned area tends to be more spatially continuous with fewer fragmented patches. Consequently, features such as the edge ratio, area, and area ratio exhibit smaller variations, so they have lower weights than pixel-scale and structure-scale features.

The fire intensities at the four scales are shown in Figure 5. The numbers 1–4 in the legend indicate the land surface anomaly intensity from low to high, as shown in Table 2. In the latter figures of the land surface anomaly intensity, the legends all have identical meanings to those used here and are not repeated. The structure-scale, object-scale, and scene-scale intensities consistently identify the eastern part of the study area as a region of high fire intensity. In contrast, the high-intensity area identified by the pixel-scale intensity is concentrated in regions with active flames. This discrepancy may be because the pixel values in the SWIR band, particularly in dSWIR2, are typically 2–3 times greater in areas with flames than in those with other land cover types. Because dSWIR2 has the highest weighting among the pixel-scale features, dSWIR2 significantly influences the assessment and results in a higher fire intensity in areas with flames.

- Pixel Scale

The pixel-scale features selected for the fire intensity assessment are illustrated in Figure 6. The features dRED, dGREEN, dBLUE, and dNIR exhibit similar distribution patterns, with high-value regions in the eastern part of the study area. Moreover, dSWIR1 and dSWIR2 present notably high values predominantly in areas with flames. Since the calculation of dNBR incorporates the shortwave infrared (SWIR) band, which is highly sensitive to flames, its high-value regions are located mainly in these areas.

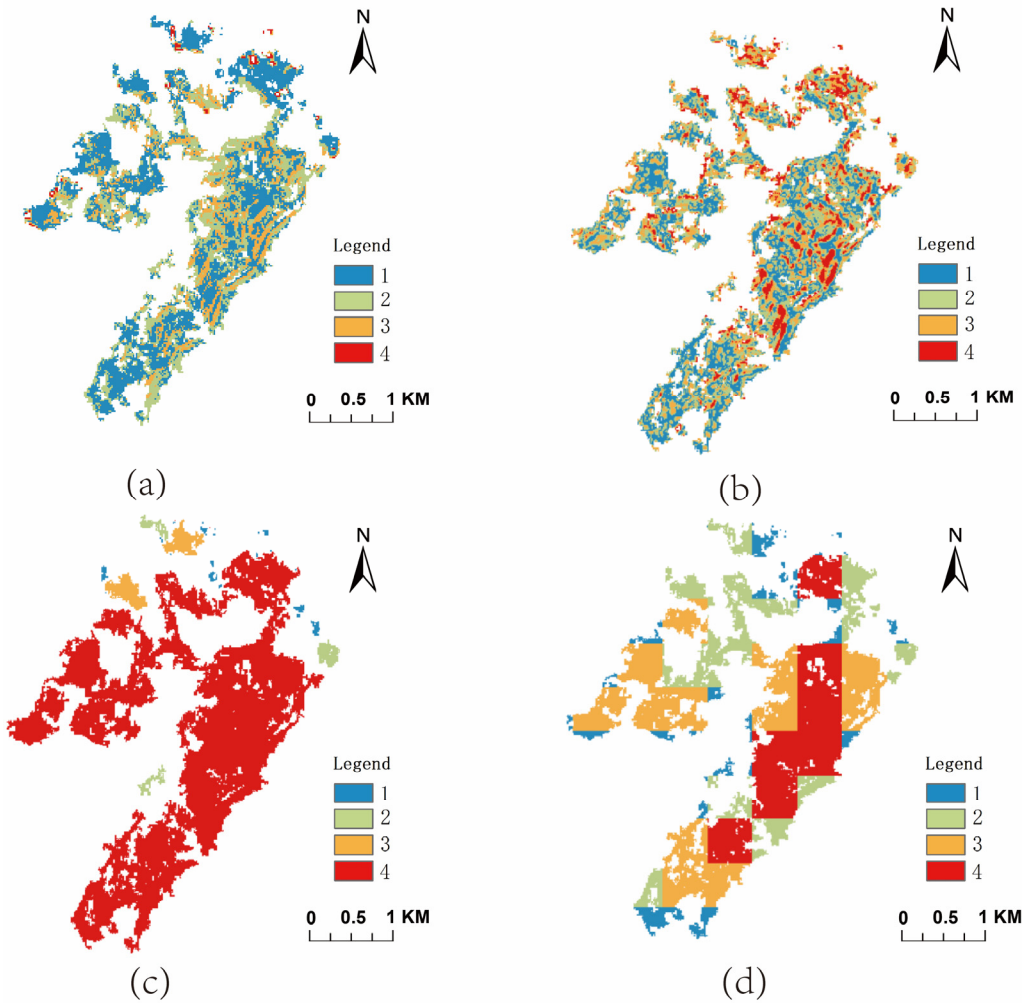


Figure 5. Fire intensities at four scales: (**a**) pixel scale, (**b**) structure scale, (**c**) object scale, and (**d**) scene scale.

As shown in Figure 7, the weight of the spectral features at the pixel scale is significantly greater than that of the scattering features. Spectral features considerably vary across burned areas. This disparity can be attributed to the fact that different fire intensities significantly change the surface colour before and after the fire. In high-intensity areas, the surface colour entirely shifts from green to black–purple, whereas in lower-intensity areas, the surface colour may change from green to a mix of green and black–purple. This change leads to larger spectral differences in regions of varying intensity, so higher weights were calculated using the entropy weight method.

Among the spectral features, dSWIR2 has a particularly high contribution. A possible reason is that during a fire, the pixel values in the shortwave infrared (SWIR) band in flame areas significantly increase, which creates a sharp contrast with those in other regions and results in a higher weight for dSWIR2.

- Structure Scale

The structure-scale features are shown in Figure 8. The features dContrast, dEntropy, dEnergy, dCorrelation, and dVariance exhibit similar spatial distribution patterns, where high values are located in the eastern and northern parts of the study area.

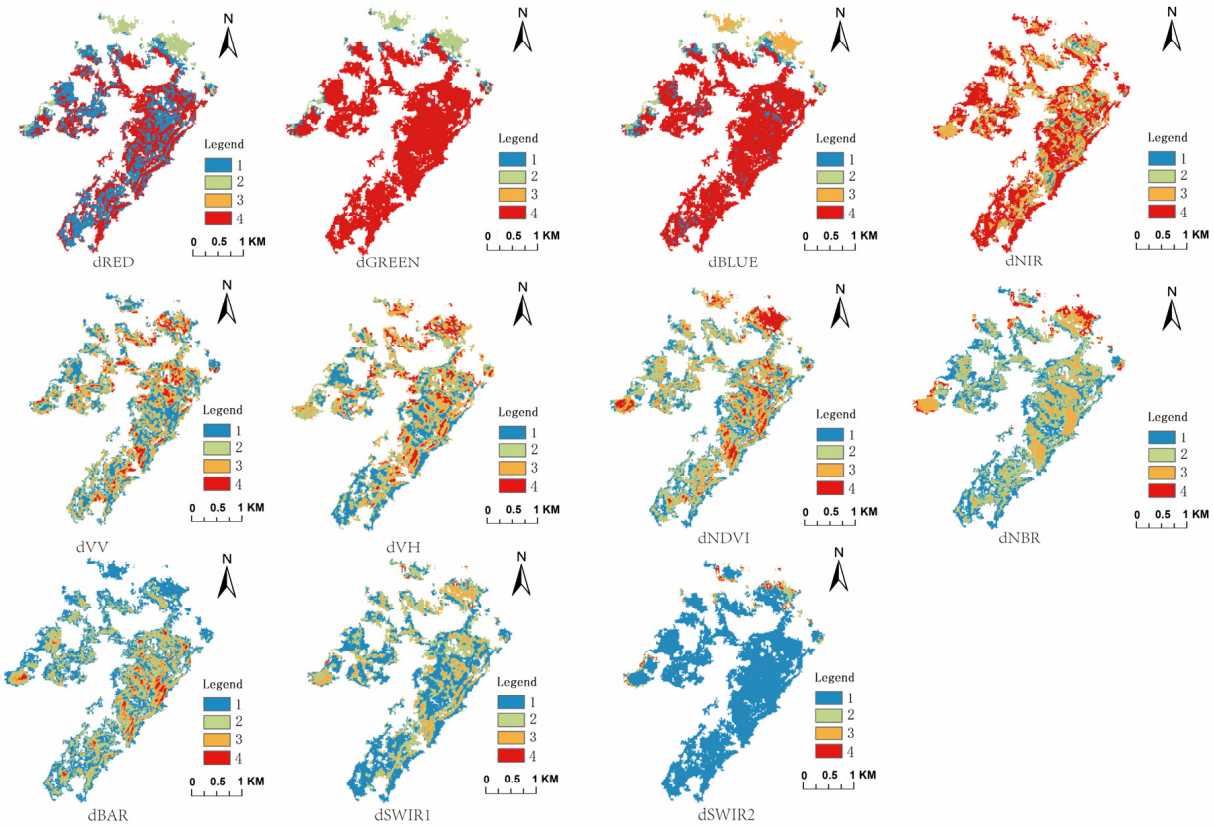


Figure 6. Pixel-scale features.

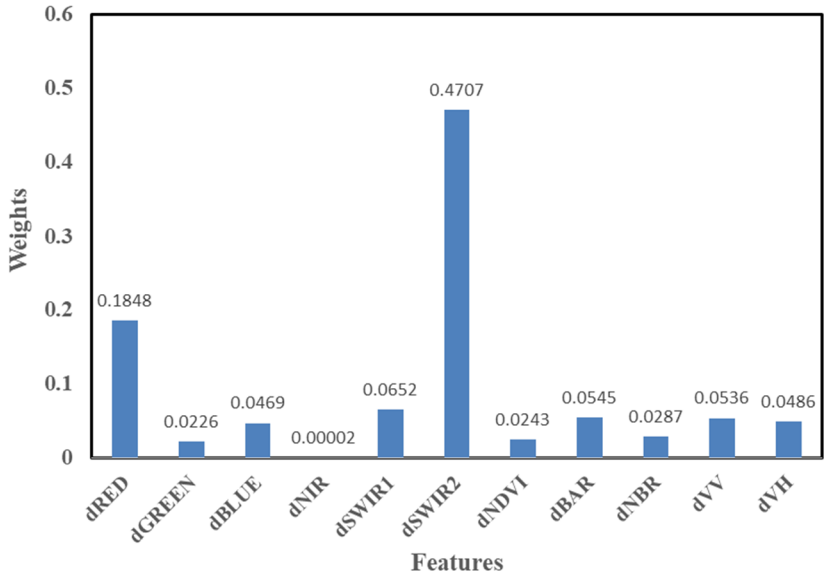


Figure 7. Feature weights at the pixel scale.

As shown in Figure 9, among the structure-scale features, dContrast has the highest weight, whereas dEntropy, dEnergy, dCorrelation, and dVariance have relatively similar weights. The reason may be that in areas of high fire intensity, severe vegetation destruction reduced the difference in image greyscale, which led to a noticeable shallowing of texture grooves. Conversely, in areas of lower fire intensity, where vegetation damage was less severe and bare ground was not fully exposed, the texture grooves were only slightly shallow, so there was a greater contrast difference between regions of varying intensity. As a result, dContrast has a higher weight.

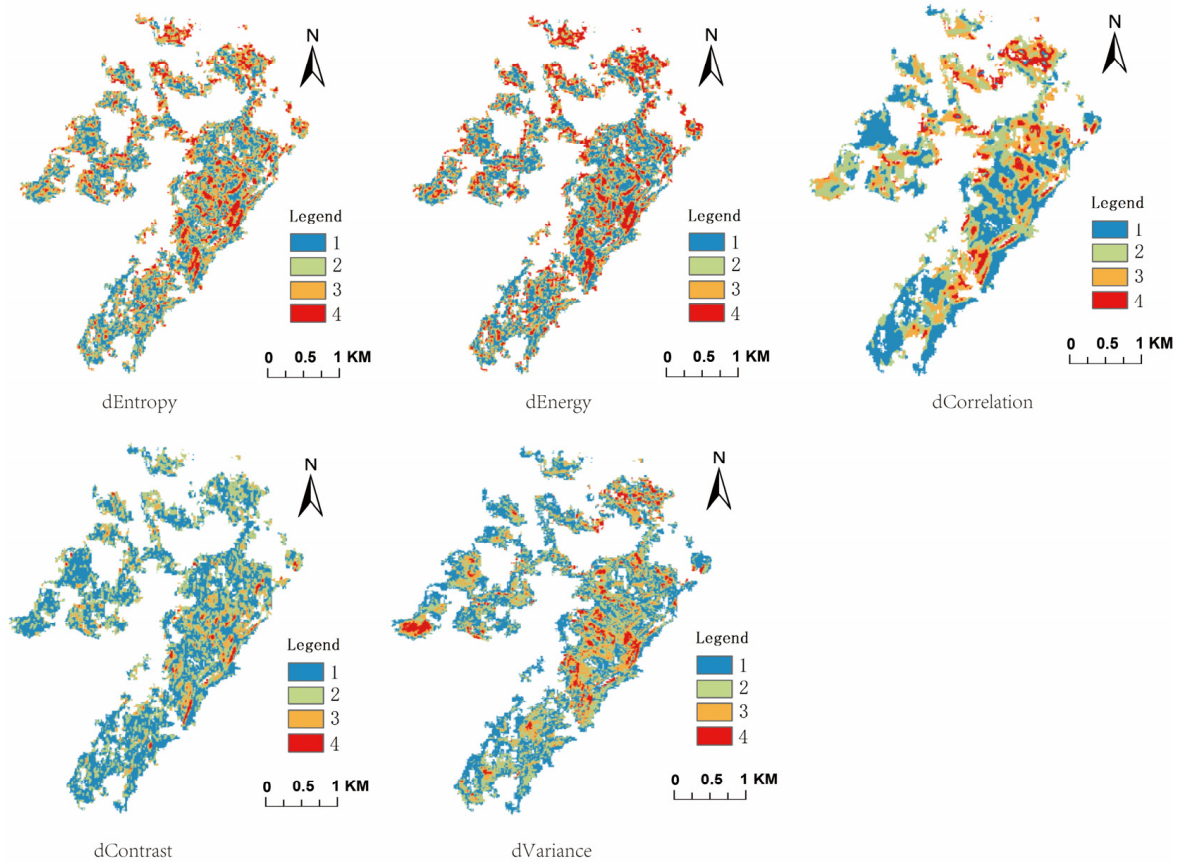


Figure 8. Structure-scale features.

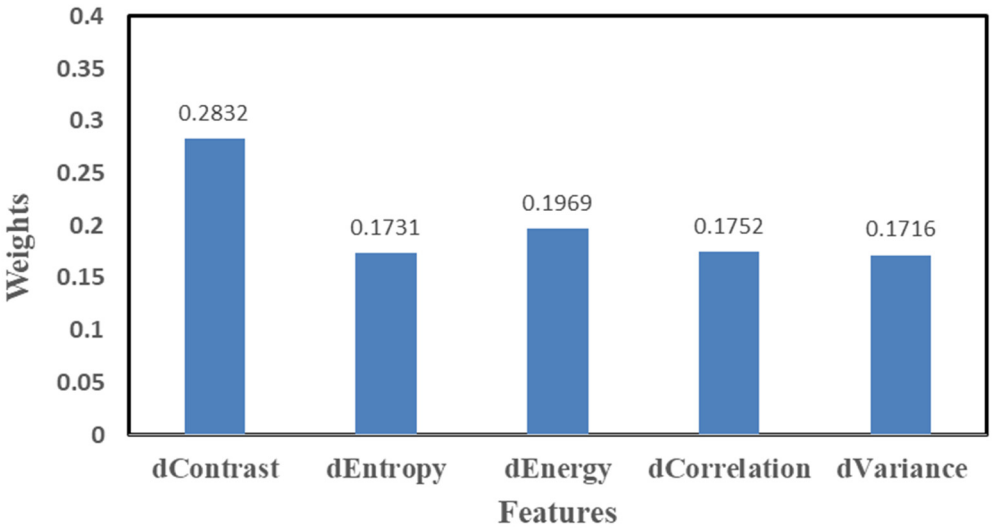


Figure 9. Feature weights at the structure scale.

- Object Scale

The selected object-scale features are shown in Figure 10. At the object scale, the edge ratio serves as a negative feature for the fire intensity assessment, whereas the area acts as a positive feature. The fire intensity results derived from the edge ratio are consistent with those obtained from the area. Both features indicate that the eastern part of the study area was characterized by high fire intensity, whereas the northern part had low fire intensity.

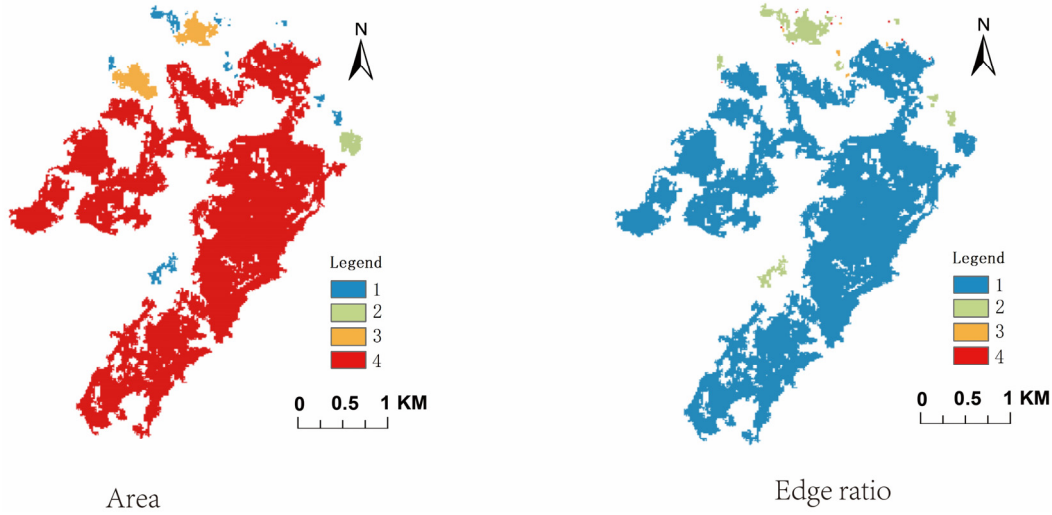


Figure 10. Object-scale features.

As shown in Figure 11, at the object scale, the area had a greater weight in the assessment, which may be attributed to the significant variations in area values. In the northern part of the study area, the burned areas were discontinuous, and the presence of smoke interference led to the extraction of numerous small, burned areas. In contrast, the eastern part of the study area experienced extensive fire spread, resulting in more continuous burned areas. This substantial difference in area across regions with varying fire intensities likely contributed to the higher weight assigned to this feature.

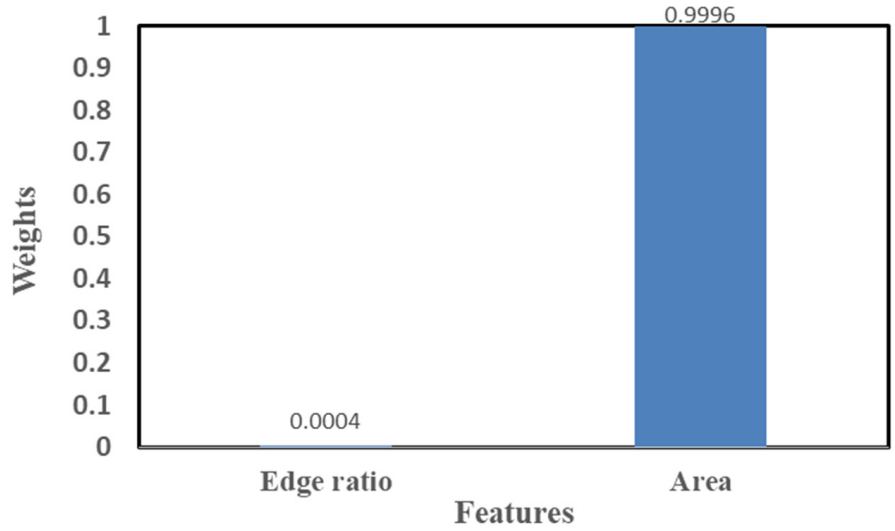


Figure 11. Feature weights at the object scale.

- Scene Scale

The scene-scale features are shown in Figure 12. The high values of the area ratio are mostly concentrated in the eastern part of the study area. This occurrence is likely due to the continuous distribution of burned areas in this region, where they almost completely occupied all grid cells and resulted in a greater proportion of burned area. In contrast, in areas such as the northern part of the study area, the burned areas were more fragmented and failed to form contiguous distributions, which led to a lower area ratio.

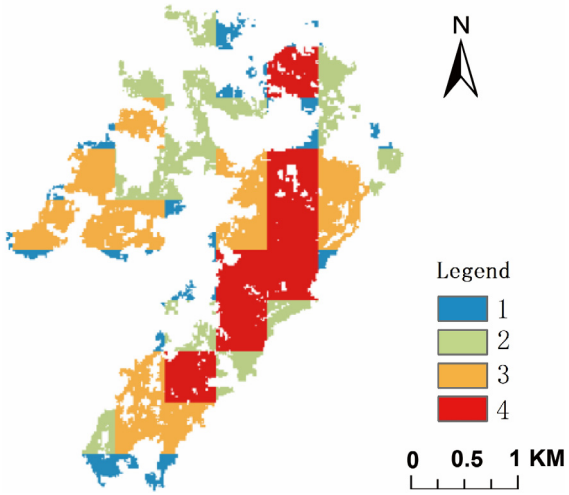


Figure 12. Scene-scale feature.

The fire intensity generated through the previous weights and features is shown in Figure 13. The areas with the highest fire intensity are located primarily in the eastern part of the study area. The inclusion of the shortwave infrared (SWIR) band highlights regions with flames as high-intensity fire regions. However, some smoke-covered areas in the northern part of the study area were evaluated as low-intensity regions, which does not align with the actual situation. This discrepancy may be attributed to the fact that while the inclusion of the SWIR band reduces smoke interference, it has limited penetration capabilities in dense smoke, so there are lower fire intensity estimates in heavily smoke-obscured areas than under actual conditions.

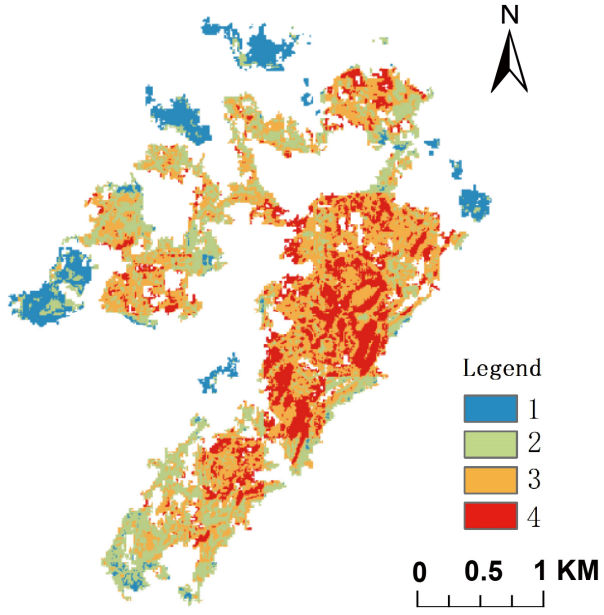


Figure 13. Fire intensity.

- Accuracy Assessment

The accuracy assessment result is in Figure 14. The overall accuracy of the land surface anomaly intensity was high (75.25%). These findings demonstrate that the proposed system in this study effectively captures and quantifies fire intensity. The assessment system developed in this study is accurate in evaluating high-fire-intensity areas. These regions are less likely to be misclassified as low-intensity areas because the pixel-scale, structure-scale, object-scale, and scene-scale features are more pronounced in high-intensity regions, so

they are easier to evaluate accurately. In contrast, lower-intensity areas are more susceptible to inaccuracies due to factors such as remote sensing image quality and shooting conditions, which lead to an overestimation of surface feature differences and intensity levels.

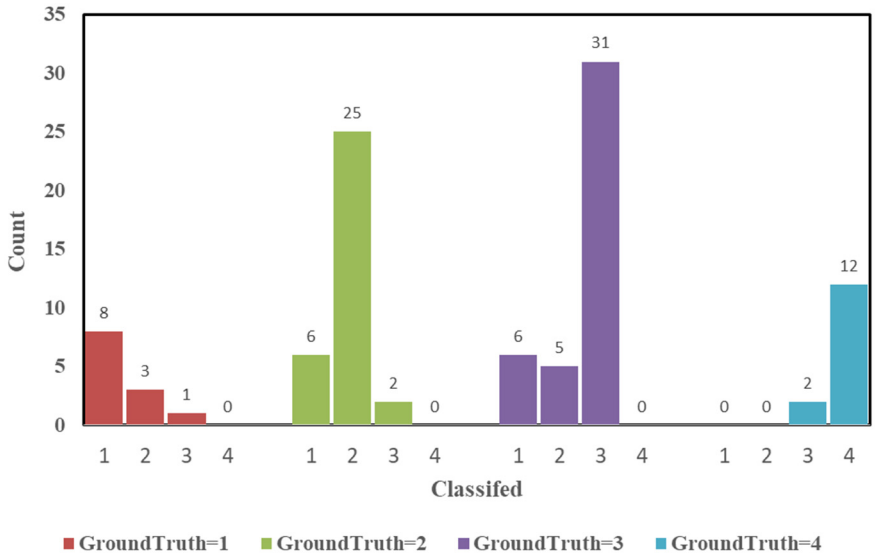


Figure 14. The assessed land surface anomaly intensity and true land surface anomaly intensity of the label points. (Classified represents the assessed land surface anomaly level, GroundTruth represents the true land surface anomaly intensity level, and Count represents the number of label points).

As shown in Figure 15, in some areas with smoke coverage, the fire intensity assessment results did not align with the actual situation: some high-intensity fire zones were evaluated as low-intensity areas. The reason for this discrepancy is that dense smoke obstructed the view, so the feature differences were underestimated for these regions, which can result in lower pixel-scale and structure-scale intensities. Additionally, smoke caused the extracted burned area to appear more fragmented, which led to lower object-scale and scene-scale intensities. Consequently, when the features from the pixel, structure, object, and scene scales were combined, the overall calculated fire intensity appeared lower than the actual ground conditions.

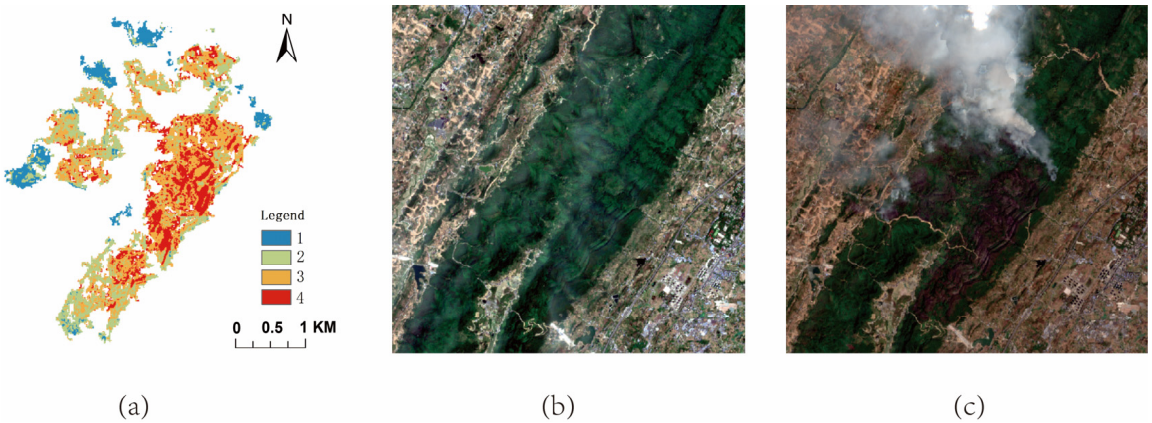


Figure 15. Assessed land surface anomaly intensity and satellite images. (**a**) Assessed land surface anomaly intensity; (**b**) pre-fire image (Sentinel-2); (**c**) post-fire image (Sentinel-2).

5. Discussion

Experiments have shown that methods for quantitatively measuring land surface anomaly intensity using multiscale remote sensing features can be used to assess fire intensity quantitatively, and the assessment results can better match real land surface

conditions. To explore the universality of the method, we applied the proposed method to other land surface anomalies, the Palu earthquake and Midwest flooding. The land surface anomalies we chose are shown in Figure 16.

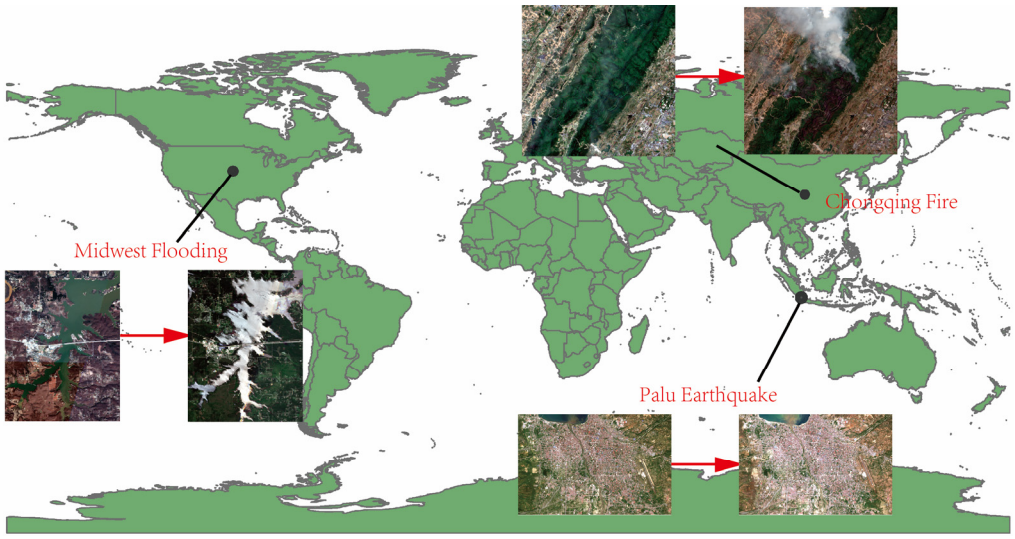


Figure 16. Selected land surface anomalies.

For the land surface anomaly intensity assessment of the Palu earthquake, the calculated feature weights were as follows: pixel-scale features: 0.1732; structure-scale features: 0.4326; object-scale features: 0.1525; and scene-scale features: 0.2417. The land surface anomaly intensity results are shown in Figure 17, and the weights of the earthquake intensity assessment feature system are shown in Table 4.

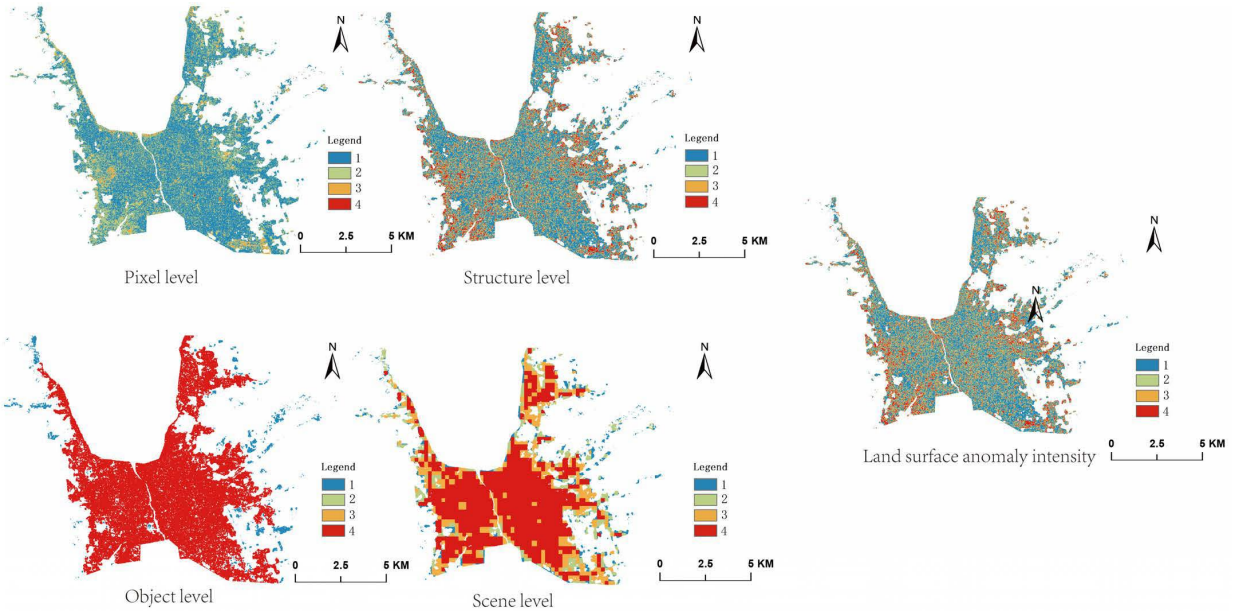


Figure 17. The land surface anomaly intensity of the Palu earthquake.

Based on empirical knowledge, earthquakes can damage buildings and surface infrastructure and significantly change surface texture features. Consequently, the structure-scale features received relatively higher weights. In contrast, since the spectral features of buildings do not significantly change before and after an earthquake and because the impact of an earthquake typically affects individual buildings or groups of buildings, the differences

at the pixel, object, and scene scales are less pronounced. Therefore, the weights for the pixel-scale, object-scale, and scene-scale features are relatively low.

Table 4. Weights of earthquake intensity assessment feature system.

Pixel Scale		Structure Scale		Object Scale		Scene Scale	
Weight: 0.1732		**Weight: 0.4326**		**Weight: 0.1525**		**Weight: 0.2417**	
Features	**Weight**	**Features**	**Weight**	**Features**	**Weight**	**Features**	**Weight**
dRED	0.0656	dContrast	0.2274	Edge ratio	0.1628	Area ratio	1.0
dGREEN	0.0634	dEntropy	0.1552	Area	0.8372		
dBLUE	0.0654	dEnergy	0.2491				
dNIR	0.0823	dCorrelation	0.1694				
dSWIR1	0.0545	dVariance	0.1989				
dSWIR2	0.0612						
dNDVI	0.0697						
dBAR	0.0186						
dNBR	0.0147						
dVV	0.2379						
dVH	0.2667						

At the pixel scale, the weight of the spectral features was relatively low. The damage to buildings and other surface facilities caused by earthquakes changed the surface roughness, so the difference in radar features was more significant, and the contribution was greater in the assessment of land surface anomaly intensity. At the structure scale, dVariance, dContrast, and dEnergy increased in weight because of the significant changes in surface grooves, which dVariance and dContrast can better reflect. At the object scale, the weight of the area was much greater than the edge ratio. The reason may be that the objects affected by the earthquake were mostly single buildings or buildings with similar morphological characteristics and more significant area differences.

The land surface anomaly intensity was compared with the real surface conditions in Figure 18. The results revealed that the overall distribution pattern of the land surface anomaly intensity was consistent with the actual surface conditions. Areas where the earthquake caused significant building collapse and vegetation damage presented relatively high land surface anomaly intensities. For example, as shown in Figure 18, the region experienced severe vegetation damage along roads after the anomaly became more intense. Similarly, other densely built areas, where numerous buildings were heavily damaged or destroyed, also presented higher intensities.



(a) (b) (c)

Figure 18. The assessed land surface anomaly intensity and satellite images of the Palu earthquake. (**a**) The assessed land surface anomaly intensity (images 1–4 in the legend indicate the land surface anomaly intensity from low to high, as shown in Table 2); (**b**) a pre-earthquake image (Sentinel-2); (**c**) a post-earthquake image (Sentinel-2).

When the accuracy assessment method is used in the accuracy assessment section, the overall accuracy of the land surface anomaly intensity assessment is 84.7%, which indicates a high level of accuracy in the intensity evaluation.

The land surface anomaly intensity assessment for Midwest flooding yielded the following feature weights: pixel-scale features at 0.3541, structure-scale features at 0.1790, object-scale features at 0.2279, and scene-scale features at 0.2390. The land surface anomaly intensity results are shown in Figure 19, and the weights of the flooding intensity assessment feature system are shown in Table 5.

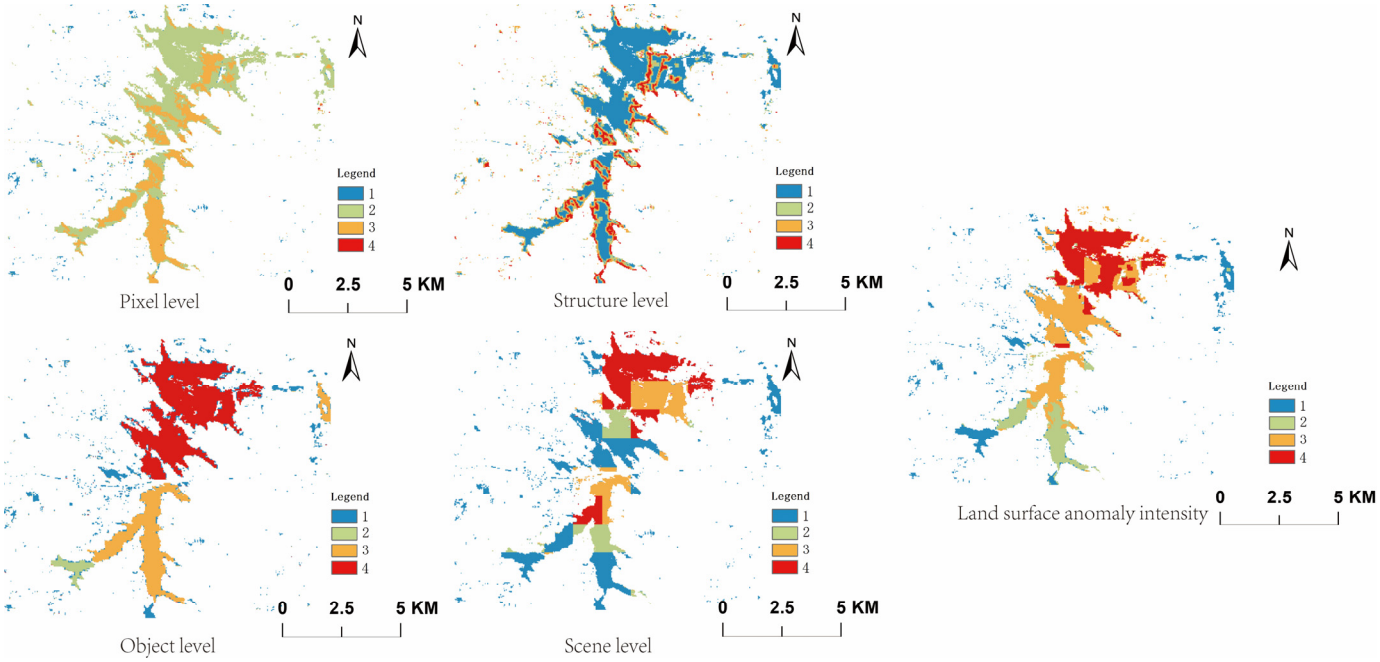


Figure 19. Land surface anomaly intensity of Midwest flooding.

Table 5. Weights of flooding intensity assessment feature system.

Pixel Scale		Structure Scale		Object Scale		Scene Scale	
Weight: 0.3541		**Weight: 0.1790**		**Weight: 0.2279**		**Weight: 0.2390**	
Features	**Weight**	**Features**	**Weight**	**Features**	**Weight**	**Features**	**Weight**
dRED	0.1374	dContrast	0.3201	Edge ratio	0.0298	Area ratio	1.0
dGREEN	0.2977	dEntropy	0.1432	Area	0.9702		
dBLUE	0.0950	dEnergy	0.1455				
dNIR	0.2401	dCorrelation	0.2012				
dSWIR1	0.0067	dVariance	0.1900				
dSWIR2	0.0032						
dNDVI	0.0289						
dBAR	0.0234						
dNBR	0.0330						
dVV	0.0779						
dVH	0.0567						

Pixel-scale features have relatively high weights. This result can be attributed to the nature of flooding disasters, where flooding submerges land, increases water turbidity, and alters the spectral characteristics of water bodies. Additionally, areas that originally exhibited land spectral features now display water spectral features. As a result, the spectral features of the land surface undergo significant changes, so pixel-scale features are more sensitive to the evaluation of the land surface anomaly intensity. Moreover, since water bodies generally maintain uniformity with minimal changes in texture, the structure-scale

features exhibited less variation and had lower sensitivity in assessing the land surface anomaly intensity.

At the pixel scale, the spectral feature weight is relatively high because flooding affects the spectral characteristics of the water body and its surrounding areas. For the structure scale, the weight of dContrast is relatively high because the grooves of the image changed after flooding part of the land. The weight of the area under the object scale is much greater than the edge ratio, possibly because the affected area of flooding was mainly a continuous surface area that spread outwards along the edge of the water. The shapes are similar, so the difference between the edge ratios of the objects is small, and the area becomes the dominant factor that affects the intensity assessment at the object scale.

The land surface anomaly intensity is compared with the real surface conditions, as shown in Figure 20. The results indicate that the land surface anomaly intensity can reflect the disaster situation. However, due to the differences in imaging time phases caused by prolonged flooding duration, some areas may exhibit erroneous land surface anomaly intensities. The observed changes in spectral and texture features in these regions might not be due to flooding but rather to differences in imaging times. This result highlights a limitation of the proposed method, which heavily relies on imagery and can capture only relative changes between two images.

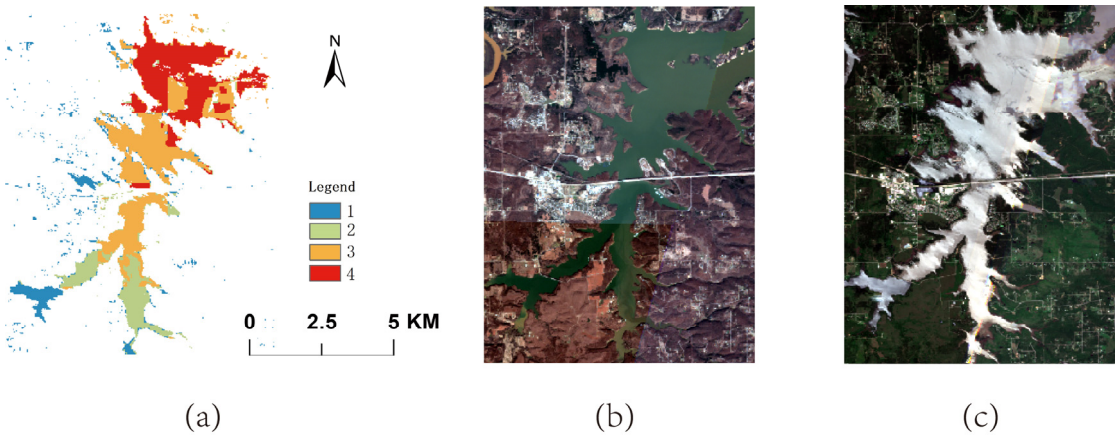


Figure 20. The assessed land surface anomaly intensity and satellite images of Midwest flooding. (**a**) The assessed land surface anomaly intensity (images 1–4 in the legend indicate the land surface anomaly intensity from low to high, as shown in Table 2); (**b**) a pre-flooding image (Sentinel-2); (**c**) a post-flooding image (Sentinel-2).

When the accuracy assessment method is used in the accuracy assessment section, the overall accuracy of the land surface anomaly intensity assessment is 82.5%, which indicates relatively high accuracy in the intensity evaluation.

Based on the above cases, the method of measuring land surface anomaly intensity using multiscale remote sensing features can be applied to assess the intensity of various land surface anomaly events. The determination of feature weights using the entropy weight method relies solely on remote sensing data without requiring additional expert knowledge or manual intervention. This approach enables adaptive adjustments of the weights of remote sensing features in different types of land surface anomaly intensity assessments. As a result, the sensitivity of various remote sensing features can be automatically adjusted according to the type of land surface anomaly being evaluated. The feature weights that are determined by the entropy weight method, which is based on mathematical principles, also align with empirical knowledge. Features that are significantly affected by land surface anomaly events are expected to play a dominant role in intensity assessment, and these features often receive higher weights when the entropy weight method is used. Conversely, less important features are assigned lower weights and have a diminished influence on enabling automated feature selection.

The proposed land surface anomaly intensity assessment framework, which is based on pixel-scale, structure-scale, object-scale, and scene-scale features, offers significant advantages and broad application prospects in quantitatively evaluating land surface anomaly intensity. In terms of early warning for surface anomalies via remote sensing, the proposed method can rapidly generate assessment results to help identify key affected areas and support efficient post-disaster rescue and recovery efforts. This method satisfies the evolving needs for the remote sensing monitoring and early warning of land surface anomaly events in disaster response, environmental emergency management, and regulatory oversight in China.

Despite the many advantages of this method in land surface anomaly intensity assessment, several limitations remain. First, land surface anomalies such as ground subsidence are three-dimensional land surface anomaly events. The changes in three-dimensional characteristics can also be reflected through the remote sensing images obtained before and after the land surface anomaly event. This method still fits our proposed definition of remote sensing-based land surface anomaly intensity detection. However, our proposed method does not consider these factors. Three-dimensional characteristics should also be included to assess different kinds of land surface anomalies. Second, the current approach primarily uses a linear expression, which may not fully capture the complexity of nonlinear land surface anomalies. Moreover, the lack of clarity in physical meaning is a major problem with the current methodology. In the future, we will continue to explore the applicability of the proposed method to other types of land surface anomalies. Our future research should also clarify the physical implications; focus on developing nonlinear methods for expressing land surface anomaly intensity; and integrate unsupervised clustering techniques, traditional machine learning, and deep learning to increase the adaptability and accuracy of assessments of nonlinear land surface anomalies.

6. Conclusions

This study developed a remote sensing evaluation framework for land surface anomaly intensity based on the pixel scale, structure scale, object scale, and scene scale. A remote sensing evaluation feature system was established to quantitatively assess the land surface anomaly intensity according to an example of a Chongqing fire. The methodology used to measure the land surface anomaly intensity was applied to other events, such as earthquakes and floods. The main conclusions are as follows:

(1) Similar to humans, which use their eyes to observe changes in the Earth's surface, remote sensing serves as a pair of eyes in space that can detect land surface changes from afar. This technology enables the monitoring of land surface anomalies, analysis of their intensity, and assessment of their impacts. Remote sensing provides a versatile tool for measuring the intensity of various land surface anomalies, so it is indispensable for understanding and addressing these phenomena.

(2) The developed land surface anomaly intensity evaluation method, which is based on the pixel, structure, object, and scene scales, effectively quantifies the land surface anomaly intensity with high accuracy. The method is particularly effective in representing the intensity of severely affected areas. Structure-scale and pixel-scale features more significantly contribute to expressing the land surface anomaly intensity.

(3) The proposed multiscale feature-based method for evaluating land surface anomaly intensity via remote sensing adapts feature weights to different types of land surface anomaly events and demonstrates broad applicability. This study provides a timely basis for decision-making in early warning systems for land surface anomalies and satisfies the need for real-time alerts in China's new era. This approach enhances proactive capabilities in emergency response, crisis management, and regulatory enforcement.

Author Contributions: S.G.: Writing—original draft, Methodology, Writing—review and editing, Data curation, Formal analysis, and Validation. J.Z.: Conceptualization, Writing—review and editing, Methodology, Funding acquisition, and Supervision. Y.D.: Methodology and Formal analysis. Q.W.: Conceptualization, Funding acquisition, and Supervision. All authors have read and agreed to the published version of the manuscript.

Funding: This research was supported by the National Natural Science Foundation of China (Grant No. 42192580 and Grant No. 42192584).

Data Availability Statement: The data presented in the study are openly available in Copernicus Data Space Ecosystem at https://dataspace.copernicus.eu (accessed on 3 November 2023).

Conflicts of Interest: The authors declare that they have no known competing financial interests or personal relationships that could have appeared to influence the work reported in this paper.

References

1. Wei, H.; Jia, K.; Wang, Q.; Cao, B.; Qi, J.; Zhao, W.; Yang, J.H. Real-time remote sensing detection framework of the earth's surface anomalies based on a priori knowledge base. *Int. J. Appl. Earth Obs. Geoinf.* **2023**, *122*, 103429. [CrossRef]
2. Qiao, W.A.N.G. Research framework of remote sensing monitoring and real-time diagnosis of earth surface anomalies. *Acta Geod. Cartogr. Sin.* **2022**, *51*, 1141.
3. Wang, Q.; Hou, P.; Zhang, F.; Wang, C. Integrated monitoring and assessment framework of regional ecosystem under the global climate change background. *Adv. Meteorol.* **2014**, *2014*, 896453. [CrossRef]
4. Yang, S. Development and prospect of disaster remote sensing monitoring system. *City Disaster Reduct.* **2018**, *6*, 12–19.
5. Tang, X.; Liu, K.; Wang, J.; Gan, Y.; Lou, L. Design and application of satellite remote sensing emergency monitoring information service framework—A case study of forest fire in Muli, Sichuan Province. *Bull. Surv. Mapp.* **2020**, *2020*, 110–113.
6. NNU_Group. Intensity of Disaster, Concept & Semantic, OpenGMS. 2011. Available online: https://geomodeling.njnu.edu.cn/repository/concept/e6fa3d31-cf2a-4d52-8a16-5c6245e4ba31 (accessed on 3 June 2023).
7. Keeley, J.E. Fire intensity, fire severity and burn severity: A brief review and suggested usage. *Int. J. Wildland Fire* **2009**, *18*, 116–126. [CrossRef]
8. Xu, Q.; Dong, X.; Li, W. Integrated space-air-ground early detection, monitoring and warning system for potential catastrophic geohazards. *Geomat. Inf. Sci. Wuhan Univ.* **2019**, *44*, 957–966.
9. NOAA-USGS Debris Flow Task Force; Atmospheric Administration. *NOAA-USGS Debris-Flow Warning System—Final Report*; US Geological Survey: Reston, VA, USA, 2005; Volume 1283.
10. Kaku, K.; Aso, N.; Takiguchi, F. Space-based response to the 2011 Great East Japan Earthquake: Lessons learnt from JAXA's support using earth observation satellites. *Int. J. Disaster Risk Reduct.* **2015**, *12*, 134–153. [CrossRef]
11. Voigt, S.; Giulio-Tonolo, F.; Lyons, J.; Kučera, J.; Jones, B.; Schneiderhan, T.; Guha-Sapir, D. Global trends in satellite-based emergency mapping. *Science* **2016**, *353*, 247–252. [CrossRef]
12. Wang, Q. Progress of environmental remote sensing monitoring technology in China and some related frontier issues. *Natl. Remote Sens. Bull.* **2021**, *25*, 25–36. [CrossRef]
13. Xia, X.S.; Zhu, X.F.; Pan, Y.Z. Study on evaluation method of natural disaster based on historical cases. *J. Catastrophol.* **2016**, *31*, 219–225.
14. Du, C.; Wang, Q.; Li, Y.; Lyu, H.; Zhu, L.; Zheng, Z.; Guo, Y. Estimation of total phosphorus concentration using a water classification method in inland water. *Int. J. Appl. Earth Obs. Geoinf.* **2018**, *71*, 29–42. [CrossRef]
15. Brewer, M.; Owen, T.; Pulwarty, R.; Svoboda, M. *National Integrated Drought Information System (NIDIS): A Model for Interagency Climate Services Collaboration*; National Academy Press: Washington, DC, USA, 2006.
16. Casagli, N.; Frodella, W.; Morelli, S.; Tofani, V.; Ciampalini, A.; Intrieri, E.; Lu, P. Spaceborne, UAV and ground-based remote sensing techniques for landslide map**, monitoring and early warning. *Geoenviron. Disasters* **2017**, *4*, 9. [CrossRef]
17. Niu, X.; Tang, H.; Wu, L. Satellite scheduling of large areal tasks for rapid response to natural disaster using a multi-objective genetic algorithm. *Int. J. Disaster Risk Reduct.* **2018**, *28*, 813–825. [CrossRef]
18. Zhao, Z.Q.; Zheng, P.; Xu, S.T.; Wu, X. Object detection with deep learning: A review. *IEEE Trans. Neural Netw. Learn. Syst.* **2019**, *30*, 3212–3232. [CrossRef]
19. Fang, Z.; Wang, Y.; Peng, L.; Hong, H. Integration of convolutional neural network and conventional machine learning classifiers for landslide susceptibility map**. *Comput. Geosci.* **2020**, *139*, 104470. [CrossRef]
20. Yang, L.; Driscol, J.; Sarigai, S.; Wu, Q.; Lippitt, C.D.; Morgan, M. Towards synoptic water monitoring systems: A review of AI methods for automating water body detection and water quality monitoring using remote sensing. *Sensors* **2022**, *22*, 2416. [CrossRef]
21. Morante-Carballo, F.; Bravo-Montero, L.; Carrión-Mero, P.; Velastegui-Montoya, A.; Berrezueta, E. Forest fire assessment using remote sensing to support the development of an action plan proposal in Ecuador. *Remote Sens.* **2022**, *14*, 1783. [CrossRef]
22. Alibakhshi, S.; Groen, T.A.; Rautiainen, M.; Naimi, B. Remotely-Sensed Early Warning Signals of a Critical Transition in a Wetland Ecosystem. *Remote. Sens.* **2017**, *9*, 352. [CrossRef]

23. Boer, M.M.; Macfarlane, C.; Norris, J.; Sadler, R.J.; Wallace, J.; Grierson, P.F. Map** burned areas and burn severity patterns in SW Australian eucalypt forest using remotely-sensed changes in leaf area index. *Remote Sens. Environ.* **2008**, *112*, 4358–4369. [CrossRef]
24. Abdallah, M.; Younis, S.; Wu, S.; Ding, X. Automated deformation detection and interpretation using InSAR data and a multi-task ViT model. *Int. J. Appl. Earth Obs. Geoinf.* **2024**, *128*, 103758. [CrossRef]
25. Imen, S.; Chang, N.; Yang, Y. Developing the remote sensing-based early warning system for monitoring TSS concentrations in Lake Mead. *J. Environ. Manag.* **2015**, *160*, 73–89. [CrossRef] [PubMed]
26. Alasali, F.; Tawalbeh, R.; Ghanem, Z.; Mohammad, F.; Alghazzawi, M. A Sustainable Early Warning System Using Rolling Forecasts Based on ANN and Golden Ratio Optimization Methods to Accurately Predict Real-Time Water Levels and Flash Flood. *Sensors* **2021**, *21*, 459821. [CrossRef] [PubMed]
27. Gao, S.; Zhang, J.; Zhou, J. Remote sensing detection of forest fires by integrating remote sensing and spatial relationship features. *J. Beijing Norm. Univ. (Nat. Sci.)* **2024**, *in press*.
28. Sharma, S.K.; Aryal, J.; Rajabifard, A. Remote sensing and meteorological data fusion in predicting bushfire severity: A case study from Victoria, Australia. *Remote Sens.* **2022**, *14*, 1645. [CrossRef]
29. Chen, S.W.; Wang, X.S.; Sato, M. Urban damage scale mapping based on scattering mechanism investigation using fully polarimetric SAR data for the 3.11 East Japan earthquake. *IEEE Trans. Geosci. Remote Sens.* **2016**, *54*, 6919–6929. [CrossRef]
30. Chen, Q.; Nie, Y.; Li, L.; Liu, X. Buildings damage assessment using texture features of polarization decomposition components. *J. Remote Sens.* **2017**, *21*, 955–965. [CrossRef]
31. Chen, J.; Liu, H.; Zheng, J.; Lv, M.; Yan, B.; Hu, X.; Gao, Y. Damage degree evaluation of earthquake area using UAV aerial image. *Int. J. Aerosp. Eng.* **2016**, *2016*, 2052603. [CrossRef]

Disclaimer/Publisher's Note: The statements, opinions and data contained in all publications are solely those of the individual author(s) and contributor(s) and not of MDPI and/or the editor(s). MDPI and/or the editor(s) disclaim responsibility for any injury to people or property resulting from any ideas, methods, instructions or products referred to in the content.